11. A. S. Jordan and R. R. Zupp, *This Journal*, **116**, 1264 (1969).
12. M. Lorenz, in "II-VI Semiconducting Compounds," D. G. Thomas, Editor, W. A. Benjamin, Inc., New York-Amsterdam (1967).
13. D. F. O'Kane and D. R. Mason, *Trans. Met. Soc. AIME*, **233**, 1189 (1965).
14. N. A. Gorjunova, V. A. Kotavich, and V. A. Frank-Kamenetsky, *Dokl. Akad. Nauk. SSSR*, **103**, 659 (1955).
15. H. Kato and S. Takanayagi, *Japan J. Appl. Phys.*, **2**, 250 (1963).
16. D. G. Thomas and E. A. Sadowski, *J. Phys. Chem. Solids*, **29**, 395 (1964).
17. R. F. Lever and F. P. Jona, *A.I.Ch.E. Journal*, **12**, 1158 (1966).
18. R. A. Reynolds, Thesis, Department of Materials Science, Stanford University (1965).
19. P. G. Shewmon, "Diffusion in Solids," McGraw-Hill Book Co., New York (1963).
20. D. T. F. Marple and M. Aven in "II-VI Semiconducting Compounds," D. G. Thomas, Editor, W. A. Benjamin, Inc., New York-Amsterdam (1967).
21. W. Albers and A. C. Aten, *Philips Res. Repts.*, **20**, 556 (1965).

GRAH-MJ 69-0520

The Effect of Oxygen Pressure on the Oxidation of Iron at 350° and 400°C

M. J. Graham and M. Cohen*

Division of Applied Chemistry, National Research Council, Ottawa, Ontario, Canada

ABSTRACT

A kinetic study has been made of the effect of oxygen pressure (10^{-6} to 60 Torr) on the oxidation of Ferrovac E iron at 350° and 400°C. The initial rate of oxidation is found to increase with increasing oxygen pressure, while after 180 min the weight gain is independent of pressure (for pressures greater than 10^{-5} Torr). Initially Fe_3O_4 forms on the surface, and once this is covered by a continuous layer of αFe_2O_3 the oxidation rate is markedly reduced. The lower the oxygen pressure, the longer the time before αFe_2O_3 starts to nucleate, and no αFe_2O_3 is observed after oxidation at very low pressures (5×10^{-6} and 1×10^{-6} Torr). An induction period is observed for the oxidation at 5×10^{-6} Torr.

The literature contains a great number of papers on the oxidation of iron [*e.g.*,(1)], but few studies have considered the effect of oxygen pressure on the oxidation kinetics. Recently Boggs and co-workers (2) have reported a study of the oxidation of zone-refined iron in the temperature range 220°-450°C, using pressures of 10^{-2} to 100 Torr. These authors find that for oxidation up to 350°C the oxide film thickness, after a given oxidation time, increases as the oxygen pressure is lowered. At 450°C, the oxidation appears to be independent of oxygen pressure. The present work examines more closely the low pressure oxidation of iron at 350° and 400°C, also extending the pressure range down to 10^{-6} Torr. The weight gains were measured using a vacuum microbalance (except for the very low pressure oxidation). The oxide phases present were identified by reflection electron diffraction and some oxide surfaces were replicated for examination by electron microscopy.

Experimental

Apparatus.—The oxidation apparatus is shown schematically in Fig. 1. A Cahn R. G. Electrobalance was mounted in a stainless steel chamber of an all metal U.H.V. system. After an overnight bake at 100°C (the maximum permissible temperature for the balance), pressures of less than 5×10^{-8} Torr were obtained, the outgassing rate of molecules from the walls, balance, etc. being $\sim 8 \times 10^{-8}$ Torr·l·sec^{-1}. The background gas as determined by a partial pressure analyzer (an A.E.I., M.S. 10 spectrometer) was mainly water vapor. To improve the vacuum capabilities of the system, all the original soldered connections in the balance were replaced by spot-welded platinum joints.

The electrobalance was used either on the 0.4 mg or 1.0 mg Recorder Range (weight change corresponding to recorder full scale deflection), with a total noise level of about 3 μg.

Low oxygen pressures were measured using Varian ionization gauges; a U.H.V. gauge for pressures below 10^{-5} Torr and a milli-Torr gauge in the range 10^{-5} to 10^{-1} Torr. These pressures were controlled by a Granville-Phillips Automatic Pressure Controller, using the ion gauges as transducers. Higher oxygen pressures were measured using an Edwards capsule dial gauge, which was installed in the gas-handling section of the apparatus.

Materials purity.—Ferrovac E[1] iron, analyzed to contain the following impurity concentrations (in ppm); Mn, 24; Si, 10; Cr, 5; O_2, 200; Ni, 11; Al, 26; Cu, 10; Co, 5; and C, 70 was used. In some of the experiments 99.997% iron (zone-refined material from the Battelle Memorial Institute[2]) was also used.

[1] Ferrovac E is the trade name of a high purity iron produced by Vacuum Metals Corporation, Division of Crucible Steel Company of America.

[2] This material was supplied through the American Iron and Steel Institute.

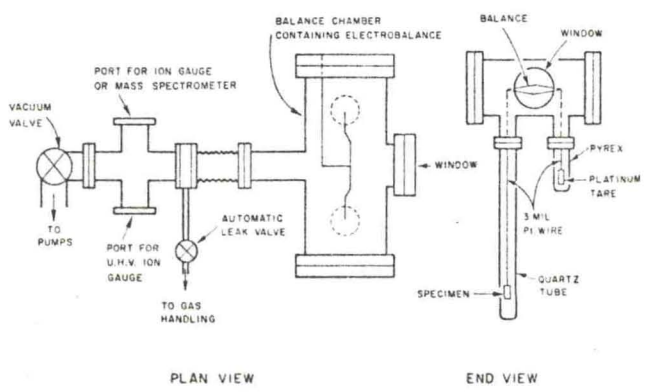

Fig. 1. Diagram of high vacuum microbalance apparatus

* Electrochemical Society Active Member.

Spectroscopically standardized oxygen and hydrogen, supplied by Baker Chemical Company were used. The oxygen contained <70 ppm total impurity and the hydrogen < 14 ppm.

Specimen preparation.—Iron coupons, 5 × 1 cm, were cut from a 9 mil thick cold-rolled sheet. They were degreased, abraded with 600 grit silicon carbide, and electropolished for 1 min in a 95% glacial acetic acid-5% perchloric acid (70%) solution (3). The specimens were then annealed in vacuum at 700°C for 2 hr and finally re-electropolished for a further minute. This method of preparation resulted in a flat surface with about 20-30Å of oxide.

Oxidation procedure.—Specimens prepared as above were first weighed on a Mettler analytical microbalance before loading into the oxidation apparatus. (The weighing of specimens on the Mettler balance before and after oxidation provided a check on the weight gain measured by the Cahn electrobalance and a small drift usually encountered with the electrobalance could be compensated for by adjusting the Cahn weight change to that given by the Mettler balance). After the system had cooled following an overnight bake, and when the pressure was $<10^{-7}$ Torr, the specimen was reduced at 600°C in about 10 Torr of hydrogen for 1 hr. After this time the hydrogen was pumped out of the system and fresh hydrogen admitted. After a few minutes this hydrogen was removed and a further dose of fresh hydrogen admitted. The system was finally evacuated and the temperature was adjusted to the value at which the oxidation experiment was to be performed. Originally, hydrogen reductions were performed at 400°C, but oxidations following reductions at this temperature gave nonreproducible results. The problem was resolved by raising the reduction temperature to 600°C.

Following the removal of hydrogen from the system, oxygen was admitted when the pressure was $<8 \times 10^{-8}$ Torr. Extra pumping time was used to reduce the background to $\sim 3 \times 10^{-8}$ Torr before oxidations were performed at the very low pressures (10^{-6}-10^{-5} Torr). At the end of an oxidation, the system was again evacuated and the weight gain was found from the difference between the initial and final weights of the specimen at the temperature of the experiment and in high vacuum. This procedure corrected for the so-called thermomolecular effect (4) which is pressure and temperature dependent and gives rise to the largest spurious mass changes encountered with the vacuum microbalance. The exact magnitude of this pressure effect was determined at the end of an oxidation experiment by re-admitting oxygen a number of times and noting the apparent mass change from the reading in vacuum. Knowing the variation of the pressure effect with time, it is then possible to accurately define the initial portion of the oxidation curve.

Oxide examination.—Reflection electron diffraction was carried out in a G. E. Diffraction Apparatus, using an accelerating voltage of 45 kV and a camera length of 50 cm. Two-stage formvar platinum-carbon replicas of the oxide surfaces were examined in the electron microscope.

Results

Kinetic data.—A comparison was first made of the oxidation of Ferrovac E iron with zone-refined iron, and the weight gain-time curves for the two materials, oxidized at 350°C and 10^{-3} Torr oxygen pressure, are shown in Fig. 2. It is observed that both materials oxidize in a similar manner for the first 10 min, after which time the rate of oxidation of Ferrovac E slows markedly while the zone-refined material continues to oxidize at a fairly rapid rate. After 2 hr, the oxide is nearly twice as thick on the zone-refined iron as on the Ferrovac E. This difference in oxidation behavior may possibly be accounted for in terms of different grain size and different crystal orientations present in

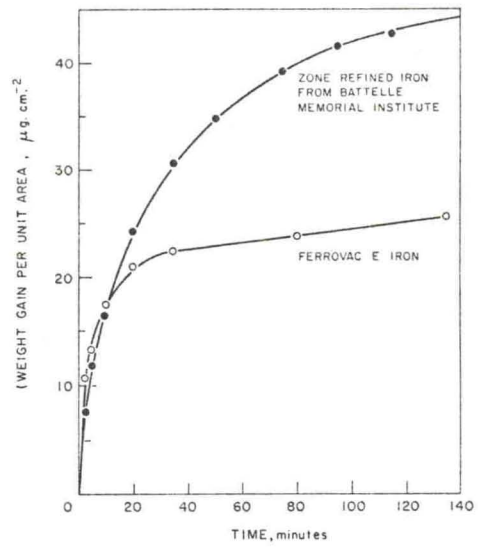

Fig. 2. Comparison of the oxidation of iron supplied by the Battelle Memorial Institute with Ferrovac E iron; 10^{-3} Torr oxygen at 350°C.

the two materials. Following the 700°C vacuum anneal, the grain size of the Battelle iron is about 2-3 mm in diameter, compared with a few microns for the Ferrovac E, and as the oxidation rate is strongly dependent on crystallographic orientation (5-7), larger grains present in the zone-refined material exposing planes with high oxidation rates may be responsible for the observed enhanced oxidation over Ferrovac E iron. Also, the time to formation of αFe_2O_3 varies with crystal plane (5), and the continued rapid oxidation observed with the zone-refined material may be taking place on large grains of such orientation that αFe_2O_3 has not yet formed a continuous film over the magnetite. The statement that a continuous outer layer of αFe_2O_3 slows the reaction rate will be discussed later. The reproducibility of oxidation runs on zone-refined iron was found to be not as good as with Ferrovac E. A series of oxidations, performed at 350°C and 10^{-3} Torr oxygen pressure on seven zone-refined iron specimens, annealed under similar conditions but some of them at different times, were reproducible to within about 10%. Specimens annealed together yielded results in closer agreement, presumably due to a more similar grain growth and grain size. Oxidations of Ferrovac E iron, under similar conditions, were reproducible to about 5%, irrespective of whether specimens were annealed at the same time or not. Because of this better reproducibility it was decided to use the Ferrovac E iron in the study of the effect of pressure on the oxidation kinetics, despite its inferior purity as compared to the zone-refined material. Also, the smaller grain sized Ferrovac E is more typical of the polycrystalline material.

The weight gain-time curves obtained for the oxidation of Ferrovac E at 350° and 400°C and oxygen pressures of 10^{-6} to 10^{-2} Torr are shown in Fig. 3 and 4, and oxidation curves for the higher pressure oxidation (10^{-2}, 35, and 60 Torr), are given in Fig. 5. In Fig. 6, a comparison is made of the very low pressure oxidation (10^{-6}, 5 x 10^{-6}, and 10^{-5} Torr), at 350° and 400°C.

Considering Fig. 3 to 6, the effect of oxygen pressure on the kinetics is clearly evident, particularly in the pressure range 10^{-6}-10^{-2} Torr. As the oxygen pressure is increased from 10^{-6} through to 35 or 60 Torr, the initial rate of oxidation is increased. The position and extent of turnover of the curves to a reduced oxidation rate is also pressure dependent. At 10^{-5} Torr and below only a small, if any, reduction in the oxidation rate is observed (with the exception of the oxidation at 10^{-5} Torr and 350°C) after 3 hr of oxidation. Although the initial rate of oxidation in-

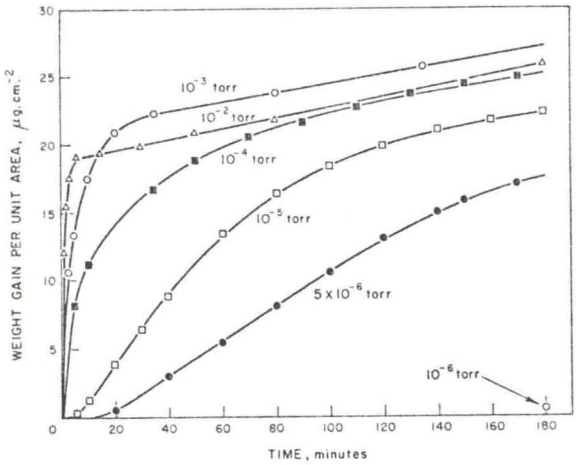

Fig. 3. Effect of oxygen pressure on the oxidation of Ferrovac E iron at 350°C.

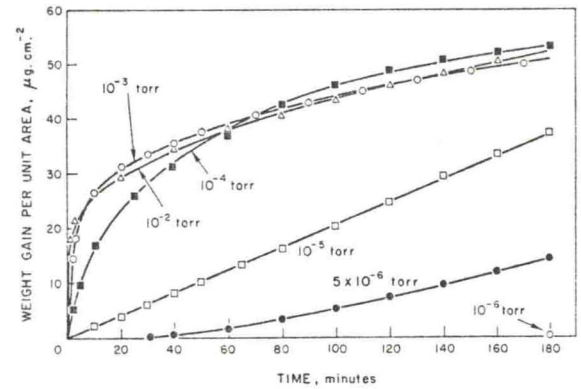

Fig. 4. Effect of oxygen pressure on the oxidation of Ferrovac E iron at 400°C.

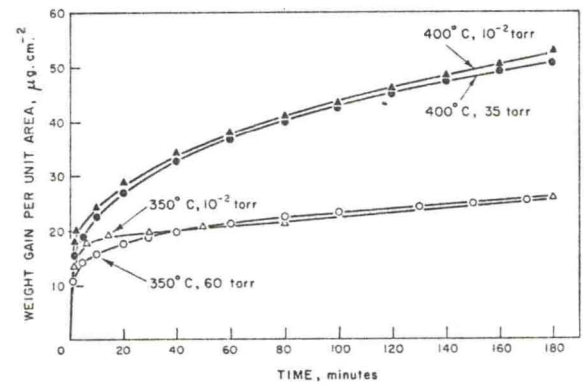

Fig. 5. High pressure oxidation of Ferrovac E iron at 350° and 400°C.

creases with increasing oxygen pressure in the range 10^{-4} to 35 or 60 Torr of oxygen, the weight gain after 3 hr is essentially pressure independent, as summarized in Table I. After 3 hr oxidation at 350°C, the average weight gain for this pressure range is about 26 μg cm^{-2}, compared with a value of about 52 μg cm^{-2} at 400°C. An induction period is observed for oxidations at 5 x 10^{-6} Torr at both 350° and 400°C.

Table I. Weight gain per unit area after 3 hr oxidation

Pressure, Torr	Weight gain (μg cm^{-2}) after 3 hr (a) 350°C	(b) 400°C
10^{-6}	~0.5	~0.1
5 x 10^{-6}	17.0	14.2
10^{-5}	22.6	37.0
10^{-4}	24.8	53.2
10^{-3}	27.3	51.0
10^{-2}	25.8	53.0
35	—	50.9
60	25.1, 25.0, 25.8	—

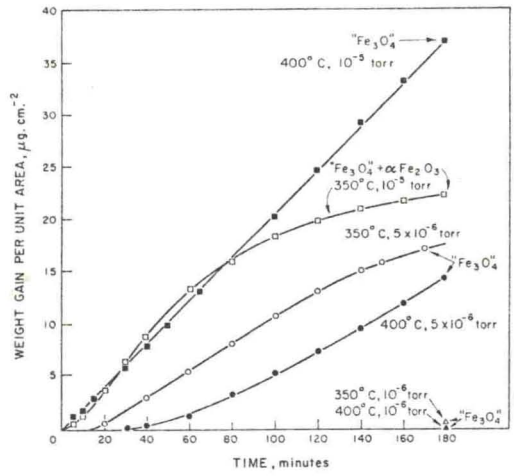

Fig. 6. Comparison of the low pressure oxidation of Ferrovac E iron at 350° and 400°C.

The weight gains after 3 hr of oxidation at 10^{-6} Torr were obtained by difference from the weight of the specimen before and after oxidation, as determined by the Mettler analytical microbalance, (taking into account the removal of the oxide film resulting from the electropolishing), the Cahn electrobalance being not sufficiently stable to identify this small weight change.

The kinetic data from oxidations at 10^{-4}, 10^{-3}, and 10^{-2} Torr oxygen at 350° and 400°C is plotted in a parabolic manner in Fig. 7 and 8, respectively. Another parabolic plot of the data from the oxidation at 35

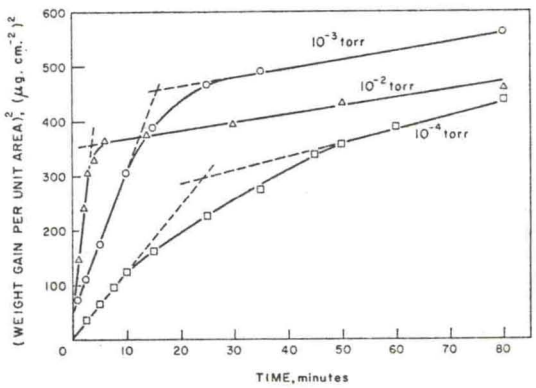

Fig. 7. Parabolic plot of data from the oxidation at 350°C; 10^{-4}, 10^{-3}, and 10^{-2} Torr oxygen pressure.

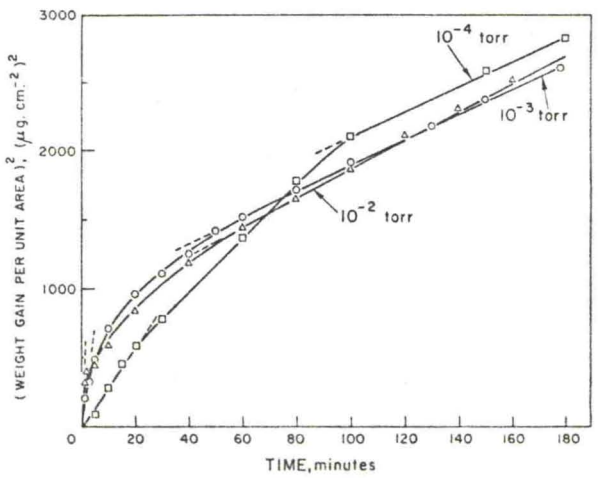

Fig. 8. Parabolic plot of data from the oxidation at 400°C; 10^{-4}, 10^{-3}, and 10^{-2} Torr oxygen pressure.

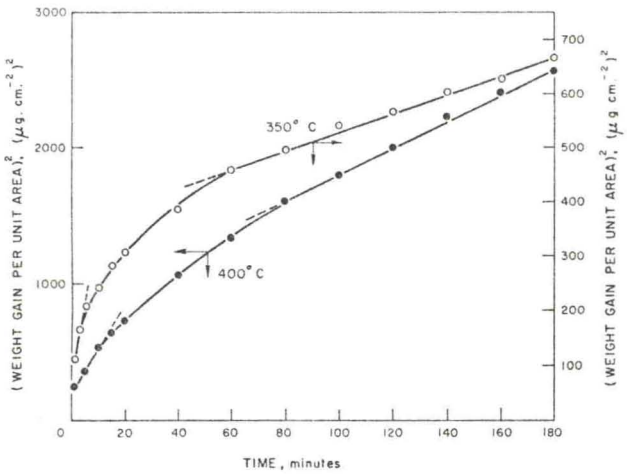

Fig. 9. Parabolic plot of data from the high pressure oxidation at 350° and 400°C.

Torr and 400°C; 60 Torr and 350°C, is shown in Fig. 9. In all cases, the initial oxidation conforms to a parabolic rate law, the duration of this period becoming shorter as the pressure is increased. The slower oxidation rate at 350°C makes the initial data for this temperature more reliable than the data at 400°C, and the time scale is expanded in Fig. 7 to show more clearly the first parabolic agreement. At the end of the first stage, the oxidation proceeds through an intermediate range before entering a second parabolic region of lower rate. It was found that the data did not fit a single logarithmic plot.

Electron diffraction.—The oxides present after oxidation, at various pressures and times at both 350° and 400°C, were identified by reflection electron diffraction and the results are summarized in Table II. "Fe_3O_4" in the table represents a cubic oxide, either Fe_3O_4 or γFe_2O_3, or both. Where αFe_2O_3 was detected (with the exception of the oxidation at 10^{-5} Torr and 350°C), this layer was too thick to permit reflections from the underlying Fe_3O_4 layer.

It can be seen from Table II that only a cubic oxide is formed at oxygen pressures below 10^{-5} Torr for both 350° and 400°C, while after 3 hr of oxidation at 10^{-4} and above, an outer layer of αFe_2O_3 is formed at both temperatures. For short time oxidations at 10^{-3} Torr and 350° and 400°C, only a cubic oxide is found to be present. An interesting finding is that αFe_2O_3 (in addition to cubic oxide), is detected after 3 hr of oxidation at 350°C and 10^{-5} Torr oxygen, while no αFe_2O_3 is found after the corresponding oxidation at 400°C.

Electron microscopy.—Electron photomicrographs of replicas of metal and different oxide surfaces are shown in Fig. 10 (a to i); the average thickness of the oxide is given in parenthesis.

Figures 10 (a) and (b) show the nature of the metal surface immediately prior to oxidation, *i.e.*, after the specimen had been hydrogen reduced at 600°C, and then held at 400°C for a few hours while the background pressure was reduced to $\sim 3 \times 10^{-8}$ Torr, it was quenched to room temperature. A smooth area of the surface is illustrated in Fig. 10 (a), compared with one of the roughest areas in Fig. 10 (b). The observed thermal facetting is similar to that found by Sewell *et al.* (8) on iron surfaces hydrogen annealed at 800°C.

Table II. Summary of electron diffraction analysis

Pressure and time of oxidation	Phases observed 350°C	400°C
10^{-6} Torr, 3 hr	"Fe_3O_4"	"Fe_3O_4"
5×10^{-6} Torr, 31 min	"Fe_3O_4"	"Fe_3O_4"
5×10^{-6} Torr, 3 hr	"Fe_3O_4"	"Fe_3O_4"
10^{-5} Torr, 3 hr	αFe_2O_3 + "Fe_3O_4"	"Fe_3O_4"
10^{-4} Torr, 3 hr	αFe_2O_3	αFe_2O_3
10^{-3} Torr, 2¼ min	—	"Fe_3O_4"
10^{-3} Torr, 5 min	"Fe_3O_4"	—
10^{-2} Torr, 3 hr	αFe_2O_3	αFe_2O_3
35 Torr, 3 hr	—	αFe_2O_3
60 Torr, 3 hr	αFe_2O_3	—

Oxide nuclei present after the oxidation at 10^{-6} Torr for 3 hr at 400°C are observed in Fig. 10 (c), and the growth of these nuclei appears to be completely random. Replicas of specimens oxidized for 31 min at 5×10^{-6} Torr at both 400° and 350°C are shown in Fig. 10 (d) and (e); this was after the induction period when a noticeable weight increase could be observed with the Cahn microbalance (see Fig. 6). The influence of substrate structure on the oxidation is shown in Fig. 10 (e) where the outer texture of the oxide on the two grains is different. Large oxide nuclei are seen in Fig. 10 (d), and triangular shaped nuclei ~200Å in height are present near the grain boundary.

Surfaces of thicker oxides are shown in Fig. 10 (f to i). Figures 10 (f) and (g) show the variation of the degree of roughness of the oxide outer surface with the underlying crystal plane of the metal. The height of oxide facets on the upper left grain in Fig. 10 (f) range up to 300-400Å. The ridged structure of the αFe_2O_3 surface, found after oxidation for 3 hr at 10^{-3} Torr and 400°C [Fig. 10 (h) and (i)], is similar to that observed by Boggs *et al.* (2, 5) for oxidations under similar conditions.

Discussion

The marked effect of oxygen pressure on the oxidation of iron at 350° and 400°C is clearly shown in Fig. 3, 4, and 5. As the pressure is increased from 10^{-6} to 60 Torr the initial rate of oxidation is increased. This period of high oxidation rate is, in general, followed by one of much lower oxidation rate.

The proposed mechanism to explain the different initial rates is as follows; initially Fe_3O_4 forms on the surface and the oxide layer grows as iron ions diffuse outward through cation vacancies in the oxide. The cation vacancies are formed at the outer surface of the oxide when oxygen is incorporated into the lattice. The concentration of vacancies and hence the concentration of iron ions diffusing to the O_2/Fe_3O_4 interface depends on the availability of oxygen at the outer surface. Thus, as the oxygen pressure is increased, the concentration of vacancies is increased and so the flux of iron ions is increased leading to an increased oxidation rate. This assumes that in the low pressure region the incorporation of oxygen into the lattice to form oxygen ions is pressure dependent.

The lowering of the oxidation rate may be due to either the formation of a continuous layer of αFe_2O_3, over the Fe_3O_4, or loss of contact between the oxide and the metal. Taper sections of these thin oxides did not yield conclusive evidence of oxide separation from the metal. Moreover, the electron diffraction data, summarized in Table II, supports the argument that the formation of a continuous hexagonal oxide layer reduces the oxidation rate. At pressures below 10^{-5} Torr, where no marked reduction in oxidation rate was observed, only cubic oxide was found to be present after 3 hr of oxidation (Table II). Also specimens which were removed before the decrease in rapid rate observed at higher pressures showed only "Fe_3O_4" by electron diffraction. In all cases where a marked decrease in oxidation rate had already occurred, electron diffraction showed only an outer layer of αFe_2O_3. These observations would indicate that in the rapid rate region, diffusion, probably of cations, through magnetite is the rate controlling process, while in the low rate region, diffusion, probably of oxygen ions, through αFe_2O_3 is the controlling process. This was partially confirmed by an experiment in which iron had been oxidized into the αFe_2O_3 region and then annealed, in vacuo, to convert all the oxide to Fe_3O_4 (9). On readmitting oxygen a rapid "magnetite-type" rate was initially observed, with again a later falling off in rate characteristic of control by αFe_2O_3.

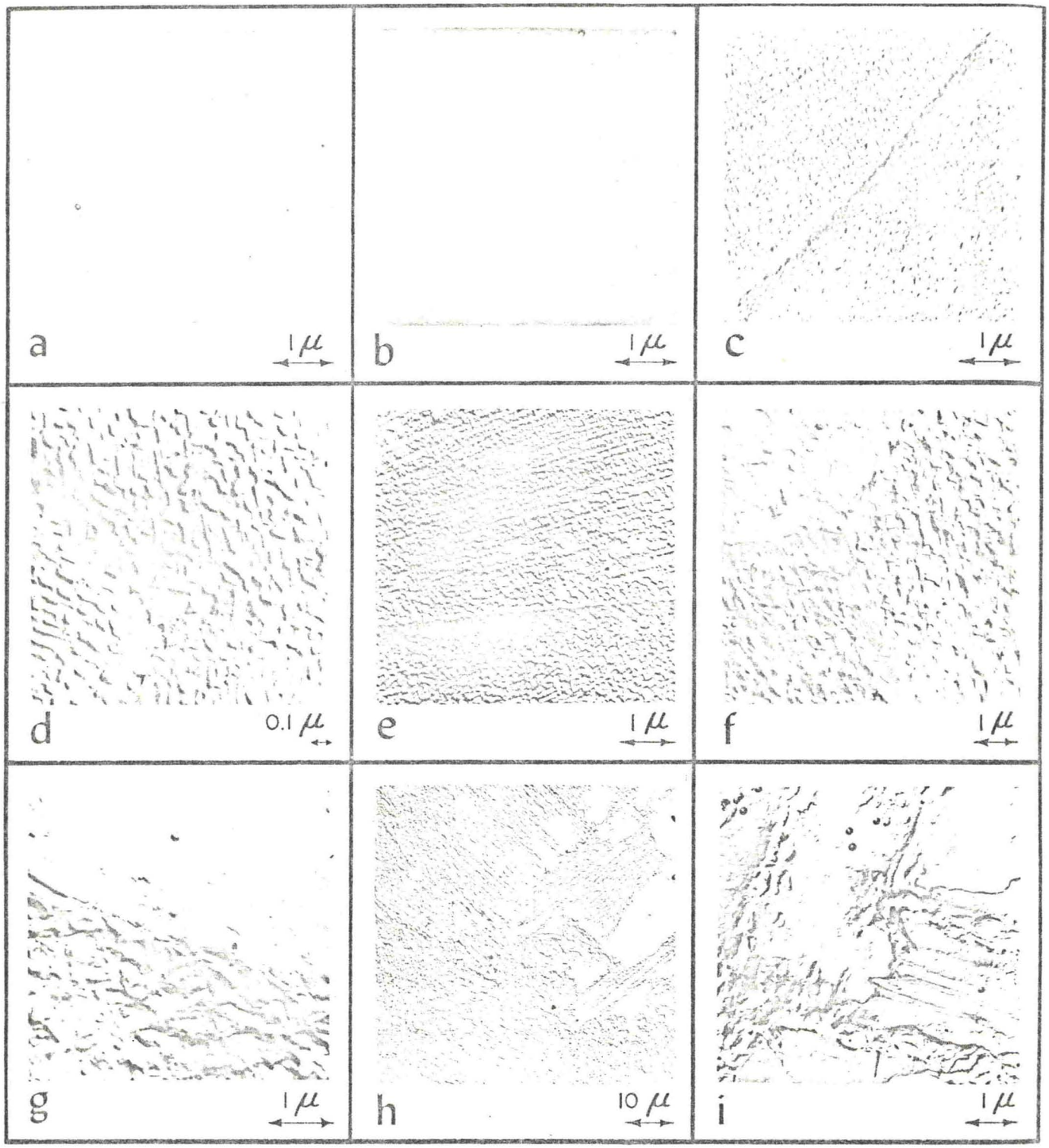

Fig. 10 (a) to (i). Electron photomicrographs of replicas of metal and different oxide surfaces; the oxide thicknesses are given in parenthesis. (a) and (b) metal immediately prior to oxidation; (c) oxidized at 10^{-6} Torr, 400°C for 3 hr (~70Å); (d) oxidized at 5 x 10^{-6} Torr, 400°C for 31 min (~50Å); (e) oxidized at 5 x 10^{-6} Torr, 350°C for 31 min (~60Å); (f) oxidized at 5 x 10^{-6} Torr, 400°C for 3 hr (900Å); (g) oxidized at 10^{-5} Torr, 400°C for 3 hr (2200Å); (h) and (i) oxidized at 10^{-3} Torr, 400°C for 3 hr (3100Å).

The time to formation of αFe_2O_3 will depend on the temperature, oxygen pressure, and crystallographic orientation of the underlying metal. The kinetic stability of an αFe_2O_3 film depends on a balance between its reduction to Fe_3O_4 by diffusing iron and the oxidation of Fe_3O_4 to αFe_2O_3 by oxygen. Thus, at 10^{-5} Torr, the higher diffusion of iron through Fe_3O_4 at 400°C leads to continuous reduction of any αFe_2O_3 to Fe_3O_4, while at 350°C a presumably slower flux of iron allows, after some time, the formation of a continuous layer of αFe_2O_3 (Fig. 6). At lower oxygen pressures only Fe_3O_4 is observed. As the pressure is increased between 10^{-5} and 10^{-2} Torr the time to formation of αFe_2O_3 is decreased. At above 10^{-2} Torr the oxidation rates are essentially pressure independent, but, of course, temperature dependent. At these high pressures αFe_2O_3 nucleates after a short time, accounting for the early turnover of the oxidation curves.

The similarity between the oxidation at 10^{-2} Torr and 35 or 60 Torr is in disagreement with the results of Boggs *et al.* (2) who report that at 350°C the oxidation rate is strongly pressure dependent over this pressure range. Although Boggs finds the initial rate of oxidation to increase as the pressure is increased,

and the present results confirm this finding over a very wide pressure range, after 150 min of oxidation he reports the weight gain with 100 Torr oxygen pressure to be about only one quarter of the weight gain found at 10^{-2} Torr. It is difficult to explain the discrepancy between the two sets of data. Part of the discrepancy may be due to the different compositions of iron used and different methods of preparation.

The reason for the induction period observed at 5×10^{-6} Torr for both 350° and 400°C is probably either to a slow nucleation process (10) taking place or the removal of oxidizable impurities, most likely carbon from the specimen. Micrographs of replicas of oxide surfaces at the end of the induction period are shown in Fig. 10 (d) and (e), where the growth of nuclei into a continuous film is taking place. As seen in Fig. 6, the induction period appears to be longer at 400°C than at 350°C, but the times involved are not sufficiently reproducible to unequivocably make such a distinction. Sewell (11) using an x-ray technique to study the kinetics of oxidation has also observed an induction period for the oxidation of (100) iron at 400°C and 3×10^{-6} Torr oxygen. It is also noteworthy that the oxide thickness determined using this new technique correlates well with the present microbalance data.

The parabolic plots shown in Fig. 7, 8, and 9 indicate two distinct regions of conformity; an initial good parabolic fit of the data, the oxidation rate increasing with increasing pressure and the duration of the agreement becoming shorter as the pressure is increased from 10^{-4} to 60 Torr. The initial parabolic behavior is followed by an intermediate stage before a second parabolic region is reached where the plots are approximately parallel, signifying that this second region is essentially independent of pressure. The two distinct parabolic rates are most clearly observed in Fig. 7, and the values of the rate constants derived from the data in this figure are the most accurate obtained; the actual values of the initial rate constants at 10^{-4}, 10^{-3}, and 10^{-2} Torr oxygen pressure and 350°C are 1.9×10^{-13}, 4.3×10^{-13}, and 1.35×10^{-12} g^2cm^{-4} sec^{-1}, respectively. In this parabolic region at 350°C and during the initial parabolic region at 400°C (Fig. 8), we are probably dealing solely with the growth of Fe_3O_4. The electron diffraction analysis of oxides formed after short times of oxidation at 10^{-3} Torr shows only Fe_3O_4 to be present (Table II), supporting this view. Thus, if initially we are only concerned with the growth of magnetite, then the rate of oxidation as given by the parabolic rate constant should be proportional to the concentration of cation vacancies at the oxide-oxygen interface, which in turn is proportional to the (oxygen pressure)$^{1/2}$. As the pressure is increased more oxygen is incorporated into the oxide and so more cation vacancies are formed, leading to enhanced diffusion of iron through these cation vacancies giving rise to an increased oxidation rate. It may be seen in Fig. 11 that for the oxidation at 10^{-4}, 10^{-3}, and 10^{-2} Torr and 350°C, the parabolic rate constant, taken from the initial slopes of the curves in Fig. 7, is proportional to the (pressure)$^{1/2}$.

Linear behavior is observed for part of 5×10^{-6} Torr at 350°C and at 10^{-5} Torr at 400°C (Fig. 3 and 4). If it is assumed that under these conditions the oxidation rate is controlled by a combination of the rate of impingement of oxygen on the surface and the sticking factor of oxygen on the oxide, a sticking factor of 0.03 at 350°C and 0.025 at 400°C can be calculated.

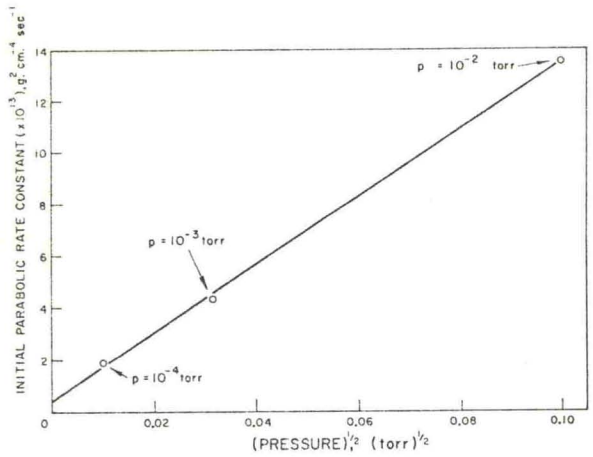

Fig. 11. Initial parabolic rate constant for the oxidation at 350°C and oxygen pressures of 10^{-4}, 10^{-3}, and 10^{-2} Torr plotted against the square root of the pressure.

Activation energies derived from the initial K_p values at 350° and 400°C, and 10^{-4}, 10^{-3}, 10^{-2} Torr are 15, 17, and 22 kcal · $mole^{-1}$, respectively. The values are obviously not too reliable as oxidation rates were only measured at two temperatures, but they are of some significance. No comparable data for oxidations under similar conditions exists in the literature but higher values of 33 kcal · $mole^{-1}$ (12), for composite oxide formation in the temperature range, 500°-900°C and 45 kcal · $mole^{-1}$ (13) for the growth of magnetite in the range 400°-570°C, are quoted for higher temperature oxidations.

Acknowledgment

The authors wish to thank Mr. G. I. Sproule for the electron microscopy.

Manuscript submitted Dec. 14, 1967; revised manuscript received July 1, 1969.

Any discussion of this paper will appear in a Discussion Section to be published in the June 1970 JOURNAL.

REFERENCES

1. O. Kubashchewski and B. E. Hopkins, "Oxidation of Metals and Alloys," Second Edition, p. 108, Academic Press, Inc., New York (1962).
2. W. E. Boggs, R. H. Kachik, and G. E. Pellissier, *This Journal*, **112**, 539 (1965).
3. P. B. Sewell, C. D. Stockbridge, and M. Cohen, *Can. J. Chem.*, **37**, 1813 (1959).
4. "Vacuum Microbalance Techniques," Vol. 1, M. T. Katz, Editor, pp. 111-150, Plenum Press, Inc., New York (1961).
5. W. E. Boggs, R. H. Kachik, and G. E. Pellissier, *This Journal*, **114**, 32 (1967).
6. M. Ramasubramanian, P. B. Sewell, and M. Cohen, *ibid.*, **115**, 12 (1968).
7. S. I. Ali and M. Cohen, Unpublished results.
8. P. B. Sewell, E. G. Brewer, and M. Cohen, *J. Phys. Chem.*, **67**, 2008 (1963).
9. E. J. Caule and M. Cohen, *This Journal*, **108**, 834 (1961).
10. J. Bénard, *Acta Met.*, **8**, 272 (1960).
11. P. B. Sewell, Unpublished work.
12. J. K. Stanley, J. von Hoene, and R. T. Huntoon, *Trans. A.S.M.*, **43**, 426 (1951).
13. M. H. Davies, M. T. Simnad, and C. E. Birchenall, *Trans. AIME*, **191**, 889 (1951); *J. Metals* (October 1951).